ACS OMEGA

http://pubs.acs.org/journal/acsodf

Article

Hydrogen Flow Controller Applied to Driving Behavior Observation of Hydrogen Fuel Cell Performance Test

Yaowaret Maiket, Rungsima Yeetsorn,* and Wattana Kaewmanee

Cite This: *ACS Omega* 2022, 7, 38277−38288

Read Online

ACCESS | Metrics & More | Article Recommendations

ABSTRACT: Fuel cell performance tests for automotive applications include static and dynamic tests, and the dynamic load test is typically carried out to investigate the cell operating performance related to driving behavior in the particular use of fuel cell electric vehicles. The automatic hydrogen flow controller, utilized to regulate the hydrogen flow as a function of time, is one of the imperative apparatuses applied for the dynamic test. The driving behavior generally consists of rapid load fluctuations, several loads running at idle, full power, overload circumstances, start−stop repeats, and cold starting, and these dynamic variations are directly related to the power required for propelling a vehicle and the demand for hydrogen volume fluctuation throughout time. The desired automatic hydrogen flow controller was designed and manufactured for the dynamic performance test via the driving simulation protocol of a heavy-duty vehicle. The main experimental activities were performed to observe the responsibility and accuracy of the invented controller. The relation between the reliability of using the automatic hydrogen flow controller and the performance improvement of fuel cell operation was studied to gain ideas for further fuel cell modification. The hydrogen flow rates controlled by the created flow controller presented a data tolerance of approximately 0.84% which was not significantly different from the theoretical figure based on T-test analysis. The controller reacted to variations in flow rates in as little as 1−2 s, which was acceptable for the dynamic test. Regarding the performance enhancement, this automatic hydrogen flow controller assisted a single cell to generate 16% more power and 33% more energy at 45 mA as a minimum current demand in comparison with the results obtained from a test system using a traditional hydrogen controller with a constant flow rate.

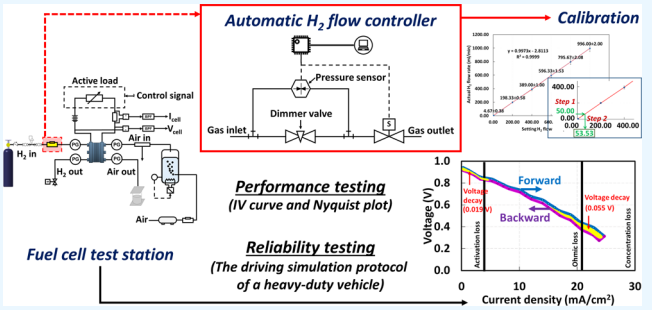

INTRODUCTION

Many automotive companies throughout Europe, North America, and Asia-Pacific, officially launched fuel cell electric vehicles (FCEVs), such as Honda Clarity fuel cell, Toyota Mirai, Hyundai Nexo models, BMW hydrogen SUV, and the Nissan X-trail.[1,2] The proton exchange membrane fuel cell (PEMFC), which is a primary energy source that generates energy via electrochemical reactions using hydrogen as a fuel, was utilized to power these cars. When compared to other electric vehicles, FCEVs have a quick refueling time of roughly 5 min. Furthermore, fuel cells have a high specific energy (590 Wh/kg),[3] high energy density (1000 Wh/L),[4] and high specific power (1600 W/kg).[5] The use of hydrogen fuel cells in heavy-duty vehicle applications is a sound decision. PEMFCs are used as a generator in heavy-duty vehicles because they provide a long operating range and good power balance. Nikola truck types, Hyundai Xcient fuel cell trucks, and Toyota-Kenmore fuel cell trucks are well-known heavy-duty FCEVs used in logistics.[6,7] In practice, the demand for energy from fuel cells will be determined by the vehicle's propulsion behavior; that is, as the vehicle's speed changes, the amount of electric power required from the fuel cell to drive the motor will fluctuate as well, increasing the demand of reactant gases, especially hydrogen. This implies that the driving behavior as a dynamic operation refers to the variation of hydrogen consumption to create electrochemical reactions. The mentioned driving behavior generally includes sudden load, start−stop, full-power driving, and overload condition. Sudden load variations in vehicle speed over time frequently occur when driving or changing lanes, while full power refers to driving a vehicle at full throttle.[8] The overload conditions happen when a vehicle is driven beyond its power capacity, and several loads running at idle are parked while the vehicle starts but does not drive. The start−stop repetitions are related to the starting and stopping of a vehicle, especially driving in a traffic jam situation. Cold starting refers to starting the engine at low

Received: April 1, 2022
Accepted: October 10, 2022
Published: October 17, 2022

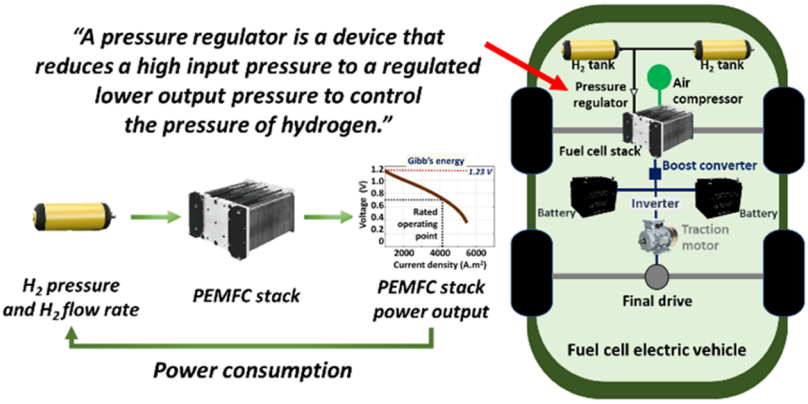

Figure 1. Fuel cell electric vehicle powertrain.

temperatures, so this situation is unlikely to occur in a tropical country like Thailand.[9]

When considering the fuel cell deployment from the powertrain configuration of FCEVs (Figure 1), it was discovered that the electric power generation of a fuel cell is caused by hydrogen fuel electrochemically reacting with the air inside the fuel cell by the vehicle's fuel supply system. A fuel cell is a high-pressure hydrogen tank containing hydrogen. It will pass through the pressure regulator to control the amount of gas using the principle of reducing the pressure between the outlets from the high-pressure tank to reduce the pressure when leaving the pressure regulator.[10]

The major advantage of an automatic hydrogen flow controller is to support a fuel cell for generating cell voltage to meet the load demand via adjusting the hydrogen supply to the fuel cell. This is because hydrogen flow regulation is related to the adjustment of an electrochemical reaction rate. If the load demand fluctuates from the application behavior, the automatic hydrogen flow control gradually adjusts the hydrogen concentration inputted into the fuel cell. Thus, the fuel cell can produce a voltage output that is appropriate for the real application. In terms of an EV powertrain, this phenomenon is feasible to reduce the battery size when the battery is regularly used as an auxiliary generator to support a fuel cell for controlling the voltage output.[11]

If a vehicle has a dynamic electrification demand that is determined by the vehicle's driving behavior, then the demand for hydrogen consumption should be dynamic as well to contribute to reaction efficiency.[12] This is because, as shown in Figure 2, the electric power generation mechanism of a hydrogen fuel cell is caused by an electrochemical reaction between hydrogen and air fed into the system. According to the electric power generation behavior of hydrogen fuel cells, the amount of hydrogen used as the starting fuel that undergoes oxidation to produce protons and electrons is the main factor affecting the amount of energy produced. More protons and electrons result in a large voltage difference between the anode and cathode sides, as well as increased electron mobility. As a result, fuel cells can generate more electricity. However, the capacity of power generation is also limited by the active area.[13] The hydrogen content is the practical dynamic, in which the fuel cell test system can control the amount of hydrogen entering the electrochemical reaction by controlling the hydrogen flow rate input.

On a lab scale, a flow rate control device is used to control a certain volumetric flow rate of electrochemical reactive gases,

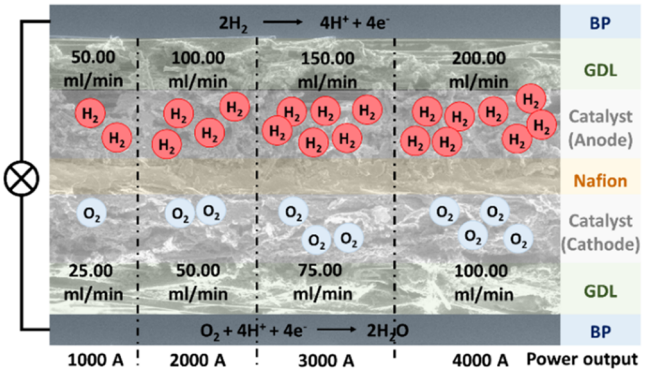

Figure 2. Mechanism of power generation of fuel cells at different reactant flow rates. Note: BP = bipolar plate and GDL = gas diffusion layer.

and this quantity of these gases is imposed based on a stoichiometric basis. Imposing a constant flow rate may lead to excess gases or lack of gases in varied demand circumstances. Thus, the capacity to alter the amount of hydrogen based on demand is a desired feature. Commercially flow control devices are available, although they are highly expensive and may have flow rate range limitations. As aforementioned, a hydrogen flow controller has been developed in this research work. The controller system can program data into the circuit to adjust the flow rate as needed. In addition, there is a function that may monitor outcomes and alter settings in real time to discover probable abnormalities and fix the workplace on time. As previously stated, flow controllers are critical in fuel cell systems because reactant flow rates can be controlled and measured based on demand. To examine the work of multifunction, the ability of the invented hydrogen flow controller has to be tested according to accuracy, responsibility, and reliability. The purpose of device accuracy testing is to calibrate the device at various flow rates. The principle of statistics, the T-test was used to examine the accuracy, standard deviation, and percentage of error as indicators of tolerance for that value. Moreover, the additional advantage related to the enhancement of fuel cell performance due to applying the invented hydrogen flow controller to the fuel cell operation system was also carried out. Performance testing is a test of the performance of a fuel cell when using a hydrogen flow controller built using the polarization curve and the Nyquist plot, and the observed results can be calculated as power parameters such as the power and voltage degradation

https://doi.org/10.1021/acsomega.2c02000
ACS Omega 2022, 7, 38277−38288

rate, and so on. The ability to put into practice and work with dynamics is referred to as reliability testing.

The dynamic operating model is thus an important factor in determining the reaction response of fuel cells via hydrogen regulation. For example, dynamic characteristics testing is a response to changes in load over time.[14,15] Figure 3 depicts the

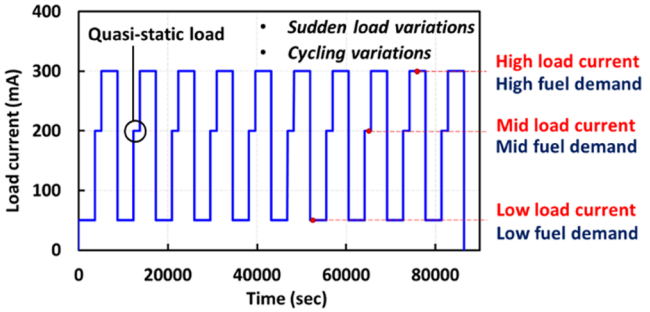

Figure 3. Example of a dynamic automotive propulsion protocol.

functional relationship between the fuel cell and the dynamics test. It was discovered that the electricity demand is unstable; the change increases and decreases over a specified period, and there is a cyclical change in which, while changing from one charge of electricity to another, hydrogen is used in various reactions.[16]

Three main hydrogen flow controllers are technically applied for supplying reactant gases to hydrogen fuel cell systems. An ultrasonic flow rate controller uses a sensor to detect ultrasonic waves reflected off the pipe surface at angles other than the flow direction, as well as a pressure differential flow controller that uses a sensor to monitor the pressure difference. The third type is the thermal flow controller that uses a bypass pipe rolled by a heating coil.[17] This research focuses on the principle of using differential pressure to create an automatic hydrogen flow controller (Figure 4), which has the advantage

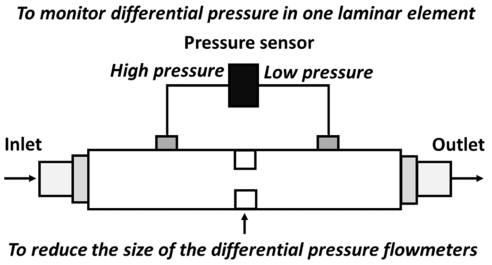

Figure 4. Device controls the differential pressure flow meter.

of being able to measure accurately with 1% RD while also responding slowly when necessary. The response speed is used as one of the factors in determining whether it influences practical application in fuel cell systems when compared to other flow regulators.

The goal of this research is to design and build an automatic hydrogen flow controller that will be used as a controller for hydrogen diffusion into electrochemical dynamics, which must produce enough electrical energy to run the simulated protocol. Based on the successful bus driving behavior, the device was tested in three stages: accuracy testing, performance testing, and reliability testing. As a result, once the hydrogen flow controller for the efficiency of the dynamic test system is finished, the hydrogen fuel consumption can be optimally controlled, allowing the research data to be used to improve the fuel cell system's efficiency, which can then be used as a foundation for future development of the use of FCEVs. The preliminary development recommendations can be drawn from the discrepancies between the efficiency test system's use of the automatic hydrogen flow controller and its real deployment in FCEVs in performance testing systems to construct protocols as needed. However, the power demand fluctuates depending on the vehicle's driving behavior, making it hard to predict whether at different times. Thus, the quantity of reactant gases should be real-time controlled related to the driving style.

RESULTS AND DISCUSSION

Accuracy Analysis of an In-House Automatic Hydrogen Flow Controller. The amount of hydrogen generated during PEMFC operation, which is the limiting reagent of the redox reaction, is a significant factor that determines power generation and voltage efficiency. The operation of a single-cell PEMFC necessitates precise and dependable flow control. The accuracy, tolerance, and responsiveness of the in-house automatic hydrogen flow controller generated by an in-house automatic hydrogen flow controller capable of managing the flow rate in the range of 0.00−1.00 L/min were investigated in this study.

The differentiation of hydrogen pressure measured from both ends of the sensor is expressed in the variation of the voltage shown by the sensor. The voltage change is directly related to control solenoid valve orifice opening and closing levels, and these levels impose the volumetric flow of hydrogen. Regarding the working principle of the created hydrogen flow controller, the voltage signal from the sensor is directly proportional to the hydrogen flow rate, and the automatic flow control mechanism is sensitive to response in 1−2 s (Figure 5). Six levels of the hydrogen flow rate were imposed to determine the precision and accuracy of the actual

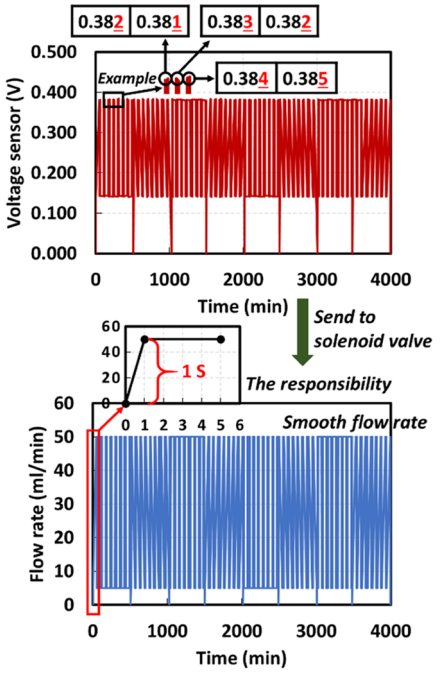

Figure 5. Response sensitivity of the in-house automatic hydrogen flow controller.

https://doi.org/10.1021/acsomega.2c02000
ACS Omega 2022, 7, 38277−38288

flow rates, and the interval of the hydrogen flow rate measurement was every minute. Figure 6 shows that the

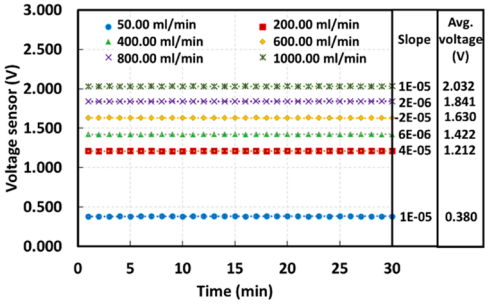

Figure 6. Relationship between the voltage sensor and hydrogen flow rates.

voltage obtained from the sensor was reasonably consistent at the same flow rate, while when the signal is provided to control the level of the hole orifice opening, it changes to the third decimal place.

The actual flow rate was compared to the imposed flow rate using the T-test, which is a statistical approach. When analyzing continuous data, a two-sample *t*-test is commonly used, however, accurate statistical inferences rely on the test assumptions being met.[18] The rational idea of applying the T-test method for the estimation of hydrogen flow controllers via observing the actual hydrogen flow rate corresponds to the need of generalization and ease of interpretation. The hydrogen flow results achieved after the *t*-test are useful for concluding if they are actually correct, and they can be applied to the entire population. The results present how different the mean of one sample is from the mean of another group. It also indicates the mean of each result from each hydrogen flow controller and the average difference between the groups of results. A larger *t*-score indicates that the results of hydrogen flow rates are different and a smaller *t*-score indicates that the results are similar.[19] The correct statistical inference is based on the test hypothesis generated by making assumptions. There are two assumptions: the primary and the secondary hypotheses. The primary assumption is the experimental flow rate that is not different from the value imposed by the computer program, and the second assumption is the value that is different from the imposed value. If the calculated *t*-value is higher than the table value (standard value), the value can reject the null hypothesis because there is no difference between means.[20] The confidence value indicating an acceptable result must be 95%. The 95% states to the level of confidence, which is the complement of the α level of significance of 0.05.[21] The *t*-value was calculated from the experimental result, corresponding to eq 1. The calculated value was −3.30, which was less than 3.18 of a confidence value (95%). It is worth mentioning that to calculate the hydrogen flow rate into the final *t*-value, the imposed hydrogen flow rates were subtracted by the measured hydrogen flow rate as the computing method in eq 1. As a result, the primary hypothesis may be accepted, while the second hypothesis can be negligible.

$$t = \frac{(\sum D/N)}{\sqrt{\frac{\sum D^2 - \left(\frac{(\sum D)^2}{N}\right)}{(N-1)(N)}}} \quad (1)$$

where t is the calculated *t*-value, $\sum D$ is the sum of the differences in the flow rate value between the actual value and setting value, and N is the amount of flow rate value.

When evaluating the tolerances of the equipment, it was found that the findings of the two analyses did not differ insignificantly; the tolerance was 0.84%, which is acceptable because hydrogen fuel consumption is generally calculated for it, according to Table 1.[17] To avoid the hydrogen deficit, use

Table 1. Featured Comparison between an In-House Automatic Hydrogen Flow Controller and Different Types of Controllers

features	flow controller types			
	in-house automatic hydrogen	thermal	ultrasonic	differential pressure
accuracy	±0.84%	±1%	±1%	±0.25%
pressure range (bar)	0−5	0−10	0−10	5−10
min flow rate (mL/min)	0	0	13	10
max flow rate (mL/min)	1000	2000	900	1500

excessive stoichiometry. Regarding oxidation basis, the stoichiometric ratio hydrogen has a stoichiometric ratio content of 1, This value was calculated using eq 2. The stoichiometric ratio of the hydrogen used in the actual oxidation reaction versus the theoretical one is expected to be 1:1

$$\text{stoichiometric ratio} = \frac{\text{mole of gas available to PEMFC}}{\text{mole of gas required for reaction}} \quad (2)$$

It indicates that there were enough hydrogen moles available to generate the needed electricity. Excess gas molecules were delivered if the stoichiometric ratio was greater than 1. A stoichiometric ratio of less than 1 can anticipate an unfavorable reaction. However, most research employs a hydrogen stoichiometry of 1.2−1.5, or 20−50% excess gas. The in-house automatic hydrogen flow controller must be calibrated to determine the correctness of the flow controller's working values. The calibration curve (Figure 7) compares the actual hydrogen flow rate value obtained from the measurement to

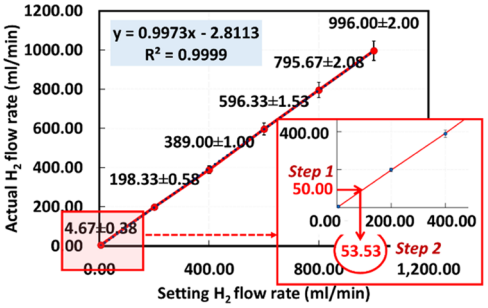

Figure 7. Hydrogen flow rate calibration curve from the in-house automatic hydrogen flow controller.

https://doi.org/10.1021/acsomega.2c02000
ACS Omega 2022, 7, 38277−38288

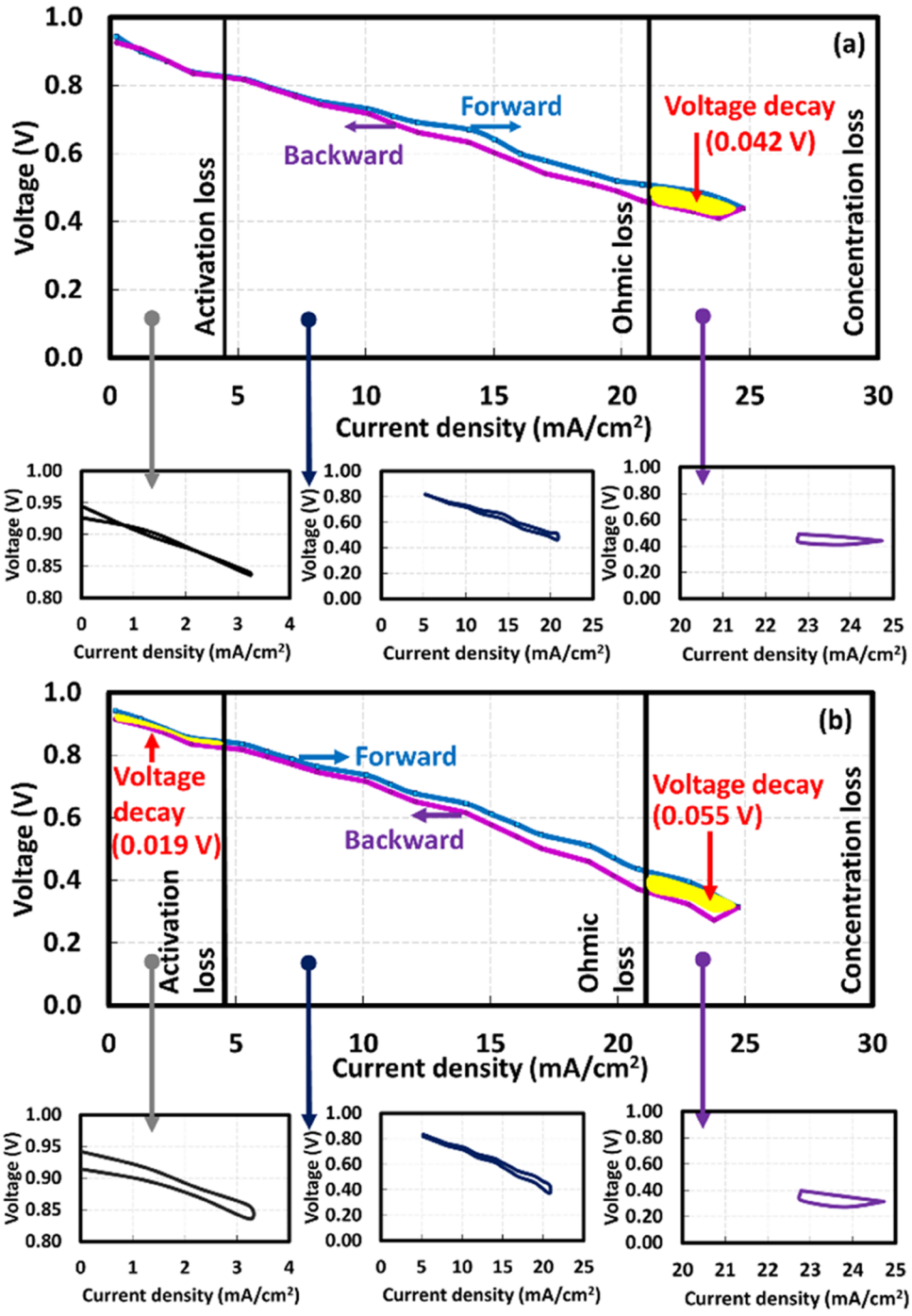

Figure 8. Hysteresis loop of the polarization curve using different flow controllers: (a) automatic flow controller and (b) static flow controller.

the value set by a computer program. According to the calibration linear line, *R*-squared is 0.9999, which represents the good validation between setting values and actual values.[22] Note, *R*-squared (R^2), is a widely used goodness-of-fit measure. As a result, in practice, the actual data from the measurement will be utilized to calculate the flow rate that will be entered into a computer program. For example, at a flow rate of 50.00 mL/min, the setting value is determined via the calibration curve by drawing a straight line from the *y*-axis at 50.00 mL/min to the straight line from the actual value, and then 53.53 mL/min is obtained by making a straight line from the graph intersection to intercept the *X*-axis. Thus, the flow rate should be set at 53.53 mL/min. This method reduces equipment failures and ensures the most precise hydrogen flow rate possible.

According to the literature,[17] thermal, ultrasonic, and differential flow controllers are typically used for fuel cell systems. Table 1 illustrates the features of different marketable hydrogen flow controllers. The criteria that were imposed to the dynamic load demand for the single cell utilized for this experiment are the optimum range of flow rates, the pressure range, and the accuracy of the flow control.

The flow rates that are typically required for the in-house test station are in the range of 0−1000 mL/min, while the pressure that is generally applied for testing the single cell or small stack is around 1−3 bar. Moreover, the created mass flow

https://doi.org/10.1021/acsomega.2c02000
ACS Omega 2022, 7, 38277−38288

controller delivered an acceptable accuracy (<1%) for flow control. The results indicate that our created hydrogen flow controller offers good promise for the performance test based on dynamic profiles.

PEMFC Performance When Using an In-House Hydrogen Automatic Flow Controller. This section of the research looked into the reliability of employing the newly developed automatic flow controller with an actual PEMFC operation. Depending on the application, PEMFC performance tests are classified into two types: static and dynamic tests. The dynamic test for automotive applications was the focus of this research. The limiting reagent, in this case, hydrogen, has a significant impact on redox efficiency and PEMFC performance. Furthermore, excessive hydrogen can lead to a build-up of charge on the catalyst surface and a large pressure drop in the system, both of which have a negative impact on the cell's performance.[23,24] In terms of how a PEMFC works, hydrogen molecules and oxygen molecules from the air mix with each other to produce an electrochemical reaction, or redox, on catalyst surfaces, and then electrons are generated. By increasing the current to the limiting current and measuring the cell voltage, the fuel cell efficiency may be estimated. The cell resistance is decreased to the open-circuit voltage to examine hysteresis characteristics. This method provides insight into a transient load, voltage losses at various current density areas, and water management in fuel cells.[25] As shown in Figure 8, the voltage losses associated with a fuel cell can be separated into three zones. The energy lost to overcome the reaction's activation energy is known as activation loss. The loss of energy induced by electron and proton resistance as they flow through the components of a fuel cell system is known as ohmic loss. Concentration loss is caused by an insufficient substrate concentration at the catalyst surface to be used in the reaction.[26,27] The main purpose of this section is to compare the efficiency and operating behavior of fuel cells using an in-house automatic flow controller to a static flow controller that can control a constant flow rate. The thickness of the hysteresis loop is determined by the polarization curve obtained from the hysteresis loop test, as shown in Figure 8. Two loop characteristics are observed in the phase 1 activation loss zone: At a current density of 0.0−0.8 mA/cm^2, the loop thickens, with the current backward lower than the current forward, implying that a lack of hydrogen for the reaction could be caused by a blockage of water in the flow channel or the gas diffusion layer, preventing it from moving to the surface of the catalyst, resulting in a voltage loss. In addition, an "8" loop and a thin loop were discovered at 0.8−3.2 mA/cm^2, indicating that the amount of hydrogen supplied to the system is sufficient for the electrochemical reaction. The appearance of an elliptical loop in the ohmic loss region can be interpreted as the ohmic loss being independent of the hydrogen flow rate; however, the activation loss due to undesirable hydrogen volumetric flow can have an impact on Gibbs free energy, which is essential for total PEMFC losses. Due to insufficient drainage from the cell, the loop appeared as a thick circle in the concentration loss scenario. Higher electrochemical reactions occur at high currents, resulting in more water generation, which must be pumped out of the fuel cell via a gas diffusion layer and a bipolar plate. As a result, if a blockage within the material prevents air from completely reacting to the redox reaction, the resulting voltage is greatly reduced.[28] When comparing the characteristics of the hysteresis loop when using an in-house automatic flow controller versus a static flow controller that can control the constant flow rate, the in-house automatic flow controllers were discovered to have thinner loops across the current density range. The static flow controller utilization can control the hydrogen flow rate as a constant. When the dynamic profile test was operated, the water quantity that exceeds the need was continuously generated and accumulated. The imbalance between the water production rate and the water removal rate led to water flooding in the cell.[29,30] Moreover, the imbalance can cause water drops inside the gas diffusion layers and gas flow channels of the bipolar plates. This circumstance can be investigated at high current demand, more than 20 mA/cm^2, when the area in the hysteresis loops is the largest. Too much water in the cell caused a decrease in electrical power generation, and it implies that the power loss is enhanced. Using an automatic hydrogen flow controller can relieve this problem.

The hysteresis loops indicated that a proper hydrogen volumetric flow bringing about an electrochemical reaction meets the dynamic load demand. The variation of hydrogen flow mainly affects activation loss that can occur in both anode and cathode catalysts. This demonstrates that using an automatic flow controller built into the fuel cell efficiency test system aids in managing the fuel diffusion phenomenon, resulting in higher fuel cell efficiency. When analyzing the functional behavior of fuel cells using the Nyquist plot (Figure 9a), it was discovered that the impedance characteristic can be

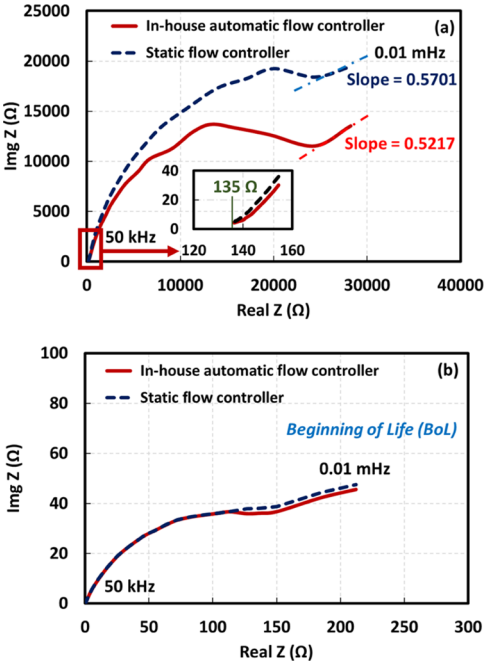

Figure 9. Nyquist plots measured via the single-cell operation (a) after profile testing and (b) BoL, using various hydrogen flow controllers.

divided into three periods. The frequencies imposed for electrochemical impedance spectroscopy (EIS) diagnosis can be separated into three regions: 1 to 50 kHz of the range at high frequency, 1 Hz to 1 kHz of the range at medium frequency, and 1 Hz to 0.01 mHz of the range at low frequency. The ohmic impedance is indicated by the first range at high frequencies. The spectral line slope is less than 45° when using an automatic flow controller at frequencies ranging

https://doi.org/10.1021/acsomega.2c02000
ACS Omega 2022, 7, 38277−38288

from 1 to 50 kHz. The spectral angle at the high frequency can be assumed as the charge that accumulates between the carbon/Nafion and carbon/water interfaces.[23,24] Since the cell resistance values obtained using both automatic and static flow controllers were the same, 135 Ω, electrochemical impedance spectroscopy was unable to identify the difference. This shows that the impedances that occur in this range are primarily due to the resistance of the components inside the fuel cell. The second half is a hemispherical spectral characteristic at medium frequencies, indicating the charge transfer resistance caused by ionic connections between catalyst layers and the membrane. This characteristic is relevant to charge transfer resistance at the cathode side. The larger loop diameter specifies the greater resistance on the cathode side, presenting that the diameter of the loop of the static flow controller is larger than that of the automatic flow controller. The hemispherical spectral characteristic and size are relevant to the charge transfer and double-layer capacitance processes occurring in the fuel cell system during the test.[31−33] The static flow controller possessed a function to control the constant hydrogen flow rate during the dynamic protocol test leading to the fuel excess phenomenon, while the automatic flow controller that can adjust the hydrogen flow rate to meet the load demand. Therefore, the fuel excess led to the mass transfer problem. Namely, the excess hydrogen flow rate removed the humidity from the fuel cell, affecting the low humidity inside the fuel cell. This phenomenon influenced the reduction of the hydration of the ionomer in the membrane. This circumstance increased the charge transfer resistance, and thus the cell performance consequently decreased. Moreover, the fuel excess led to more electrochemical reaction inside the fuel cell compared to the load demand. In terms of double-layer capacitance phenomenon that occurs when a catalyst layer on the membrane surface and a proton in the liquid solution are touching each other, causing the charges to line up and allowing electricity to be stored there, and the double-layer capacitance can increase the proton resistance affecting a decrease in the rate of charge transfer.[24,34] If the hydrogen quantity is higher than the stoichiometry demands, the positive charges can be accumulated on the surface of the catalyst layer, and then the double-layer capacitance is generated. This situation can be observed via the large diameter of the semicircle in a Nyquist plot. It demonstrates that the hydrogen supplied into the system undergoes proton dissociation in sufficient quantities to pass through the membrane to the cathode side, and thus the impedance in this range is low in comparison to the static flow controller. Excess hydrogen feeding can result in charge accumulation, increasing system resistance.[35] The third phase, which occurs at low frequencies, suggests that there are issues with mass transportation. The accumulation of product water along the flow channel, gas diffusion layer, and catalyst surface in Warburg diffusion fuel cells has been shown to create mass transfer resistance within the fuel cell. The action prevents the reactant from being transferred to the redox reaction on the catalyst surface, resulting in an incomplete redox reaction.[36] Prior to and after the hysteresis loop observation and the investigation of electrochemical behavior via EIS, nitrogen gas had been injected for 30 min for purging accumulated water in the fuel cell. It can be confirmed that the water accumulation inside the fuel cell may insignificantly have an impact on the Nyquist plot measurements. Note, during the EIS test, the fuel cell was operated at a constant current density of 0.024 A/cm^2 (0.6 A). The EIS measurement after the polarization test at the beginning of life (BoL) of the single cell including a new membrane electrode assembly (MEA) was performed in a comparison with the plots obtained from the EIS test after continuous 100-h operation. The Nyquist plots at BoL (Figure 9b) presented low charge transfer resistance, which can be observed from the size of the semicircle of the plots, whereas the ones at the end of life (EoL) illustrated high charge transfer resistance. The plots at BoL were overlayed in the region of high frequency, while in the region of mass transportation, the resistance of the cell operated with the in-house automatic flow controller was slightly lower than the one operated using the static flow controller. It implies that the different functions of flow controllers do not significantly influence the electrochemical reaction at BoL. In opposition to these apparent results, the charge transfer resistance delivered from the test after a continuous 100-h operation was principally affected by fuel consumption in the electrochemical reaction. It can be interpreted that when the fuel cell had been running continuously for 100 h, the hydrogen consumption would be required variously. The dynamic flow controller automatically adjusted the hydrogen flow rate to meet the right stoichiometry; nevertheless, the static flow controller constantly fed hydrogen into the fuel cell leading to excess hydrogen occurring in the system. The excess hydrogen was adsorbed on the activated carbon support surfaces in terms of physisorption.[37,38] Unfortunately, at 80 °C of the operating temperature in PEMFC, hydrogen cannot be desorbed from the carbon support porous surfaces, since the desorption process will occur at approximately 175 °C.[39] This phenomenon history caused the reduction in the electrochemically active surface areas (ECSAs) of a catalyst layer and the decrease in electrical conductivity of carbon support particles. Thus, the charge transfer resistance investigated via Nyquist plots was increased dramatically.

The Warburg diffusion slope is approximately 9% lower when using an automatic flow controller than when using a static flow controller. This is because the static flow controller ensures that there is more than enough fuel in the tank. The electrochemical reaction causes the reaction to run continuously, resulting in a large amount of water being produced, increasing the likelihood of water clogging. According to the data presented above, a performance test system using an automatic flow controller can handle the amount of hydrogen entering the electrochemical reaction better than a static flow controller, resulting in highly efficient fuel cells.

Ability to Implement an Automatic Hydrogen Flow Controller through Automotive Propulsion Simulation Protocols. The development of a dynamic testing station will aid in the dynamic testing of fuel cell installation capabilities. This study aims to study if fuel cells can be used as a power generator in buses that change speed according to a protocol that simulates bus driving behavior, with a particular focus on the ability to feed hydrogen into the fuel cell via an automatic hydrogen flow controller and use it as fuel for electrochemical reactions.

From Figure 10, at the same 185 mA of generated current, the voltages were in the range of 0.78−0.80 V. Considering the voltage degradation rate, it was found that the use of an automatic hydrogen flow controller resulted in it having a voltage degradation rate of 0.95 μV/h, which is 10% lower than that of a static flow controller of 1.06 μV/h. Typical values are in the range of 0.3−500 μV/h,[40] and when considering the voltage efficiency of a fuel cell, it is found that the use of an

https://doi.org/10.1021/acsomega.2c02000
ACS Omega 2022, 7, 38277−38288

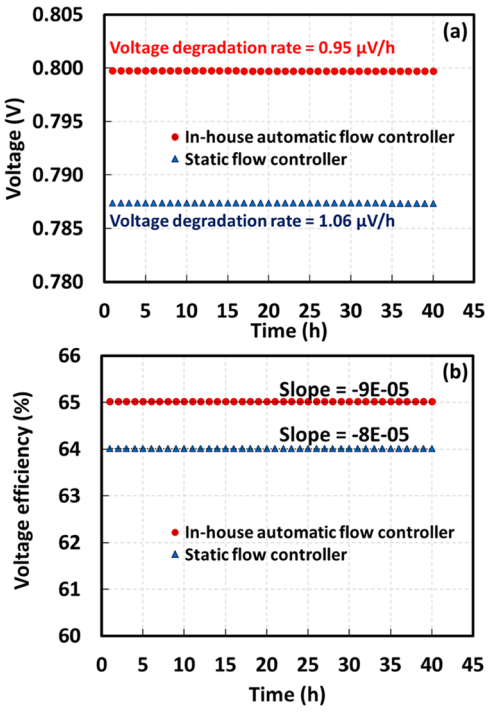

Figure 10. (a) Voltage profile at 185 mA and (b) voltage efficiency at 185 mA.

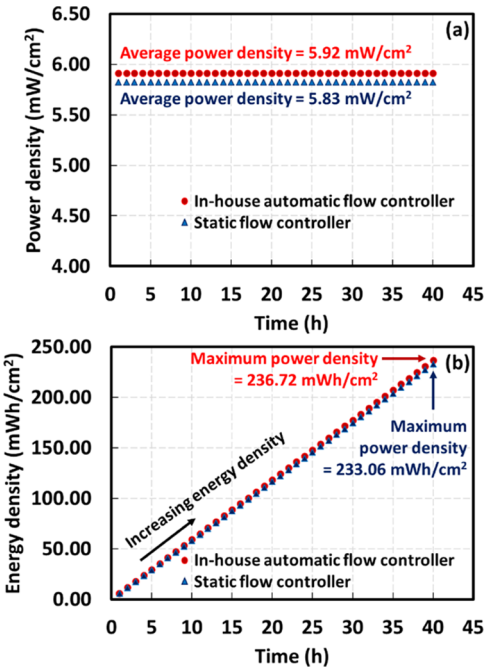

Figure 11. (a) Power density at 185 mA and (b) energy density at 185 mA.

automatic hydrogen flow controller gives the fuel cell high performance. On the other hand, when using a static flow controller, the fuel cell will have low performance, because fuel cell efficiency should be greater than or equal to 65% by standards.[41]

The capacity to generate varied voltages could be attributed to the ability to manage the amount of hydrogen utilized to react to electrochemical reactions in the system, which means that when the dynamics change, the current demand for each time period will vary and not be equal. A charge will collect on the catalyst surface if more hydrogen is given to meet the demand. The blockage of the active area creates resistance within the system, lowering the fuel cell's efficiency. The results of the diagnosis show that the traditional static flow controller failed to adequately provide hydrogen to the dynamically driven cell. When the electrochemical reaction proceeds according to the dynamic load demand, this constraint causes the depletion of the fuel reactant supply to achieve the stoichiometric basis. The power density and energy density obtained from the durability test with a certain current density support the conclusion that the automatic hydrogen flow controller is favorable for fuel cell efficiency (Figure 11). The automatic hydrogen flow controller can enable the fuel cell to produce a 2% higher average power density than the static flow controller. It has an increase in energy density production by up to 2%.

Considering fuel consumption when using fuel cells according to the 40-h bus protocol, the static flow controller uses 120 l of hydrogen, whereas the automatic hydrogen flow controller uses only 30 l of hydrogen, which shows that the use of the static flow controller leads to more energy consumption. Namely, the protocol in Figure 13 shows the current demand as a function of time. The hydrogen consumption for reacting the electrochemical reaction inside the fuel cell was different depending on the current demand. In the case of the static flow controller, it provided a constant flow rate at 0.05 L/min differing from the automatic flow controller which can adjust the flow rate depending on the protocol. This protocol required 0.05 and 0.005 L/min. So, after 40 h of testing, the static flow controller provided an excess hydrogen volume (120 l), while the automatic flow controller offered a desirable hydrogen volume (30 l). When calculating the average energy density produced by the cell (Figure 11), it was found that the automatic flow controller assisted the fuel cell to produce around 2% higher energy density than the one produced by the static flow controller. According to the performance improvement, this automatic hydrogen flow controller helped a single fuel cell to generate 16% more power and 33% more energy in comparison with the results obtained from a test system using a traditional hydrogen controller. Note that the generated power and energy were calculated at a constant flow rate at 45 mA as a minimum current demand of the test protocol. Furthermore, the static flow controller will require fuel at a cost of 144 USD. Since the automatic hydrogen flow controller only costs 36 USD to operate, it can be inferred that it is cost-effective in terms of energy management and fuel value. It can also be used in systems for dynamic performance testing. Table 2 illustrates the comparison between the automatic hydrogen flow controller, which is newly created, and the static hydrogen flow controller, which has been used for all test activities in our research group. The criteria for consideration address the fuel cell performance test related to a dynamic load demand.

CONCLUSIONS

The performance of a PEMFC operating under dynamic conditions is successfully improved in this work using an in-house automatic hydrogen flow controller. During dynamic stress testing, the controller can mitigate the issue of insufficient hydrogen fuel. This controller, for example, reduces charge accumulation on the catalyst surface and pressure drop inside the PEMFC, resulting in greater cell efficiency.

https://doi.org/10.1021/acsomega.2c02000
ACS Omega 2022, 7, 38277−38288

Table 2. Performance Comparison between the In-House Controller and the Static Controller on the 40-h Bus Protocol, after a Continuous 100 h Operation

	hydrogen flow controllers	
criteria	automatic hydrogen flow controller (in-house)	static hydrogen flow controller
amount of H_2 from H_2 tank (l)	30	120
responsibility	fast note: the flow can be adjusted by the computational program based on a test profile	slow note: the flow must be adjusted manually
effect on actual operating conditions	less	more (over stoichiometric, overpressure, more water production)
energy consumption	24 V/148 mA	24 V/148 mA
cost (USD)	low (840)	high (1400)

Furthermore, it is the main apparatus that allows for a flexible protocol design, allowing for a variety of performance test plans that is appropriate for actual use, particularly for FCEVs.

We designed and built an automatic hydrogen flow controller for controlling the amount of hydrogen in the fuel cell dynamic test station. It is capable of managing the flow rate in the range of 0.00−1.00 L/min. According to the *t*-test analysis, the accuracy is acceptable, with a tolerance of 0.84% and a sensitivity to response in 1−2 s. The in-house automatic hydrogen flow controller can control the amount of hydrogen sufficient to meet the dynamic fuel cell power generation needs. It has a voltage efficiency of 65% and a degradation rate of 0.95 μV/h, which is within acceptable standards. Moreover, the in-house automatic hydrogen flow controller can also manage fuel more efficiently, reducing fuel consumption by up to 75% compared to using a static flow controller. It can be concluded that the in-house automatic hydrogen flow controller can be used in the fuel cell dynamic test station and can apply the knowledge of fuel management that will be further developed for use in FCEVs in the future.

EXPERIMENTAL METHODOLOGY

Proton Exchange Membrane Fuel Cells and Their Performance Testing Conditions. The in-house single-cell proton exchange membrane fuel cell (PEMFC) contains the following design components: (i) The membrane electrode assembly is made of Nafion type 212, with a size of 49 cm^2. (ii) The catalyst is made of platinum catalysts supported by carbon 0.40 mg/cm^2 (40%). The active area on both the anode and cathode sides was 25 cm^2. (iii) On both the anode and cathode sides, a carbon paper Sigracet 28 BC gas diffusion layer is used, (iv) graphite plates are used to make bipolar plates, and (v) copper plates are used as the current collector. With a force of 4 Nm, each component is assembled. Once the fuel cell is assembled, it will be tested for the fuel cell's performance with the efficiency test system shown in Figure 12. The test used 99.99% pure hydrogen as the fuel and humidified air as an oxidizing agent via a humidifier. The operating conditions are: the stoichiometric ratio of hydrogen to air is 2:1; the operating temperature is 30 °C; the system pressure is 1 atm; and the relative humidity is 100%. The stoichiometric content of hydrogen and air, temperature, and pressure are the main

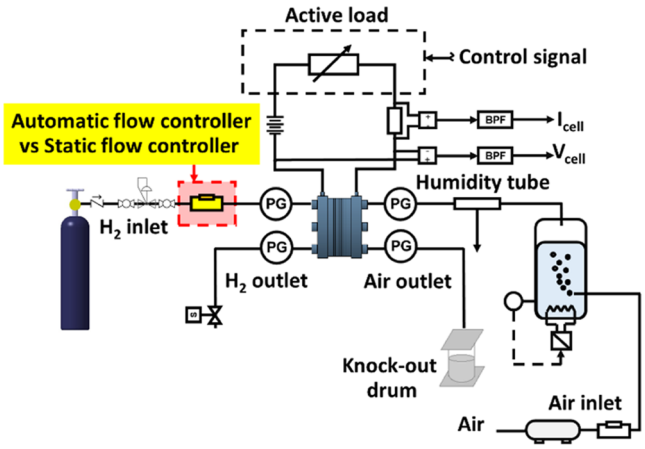

Figure 12. Fuel cell performance test station.

parameters of such tests. Choose an appropriate value from the thermodynamic data's enthalpy and entropy. The Grotthuss proton transfer mechanism[42,43] was used to determine the optimal relative humidity. Preliminary fuel cell efficiency testing revealed that the generated fuel cell was capable of producing a maximum power output of 200 mW at 450 mA of current and 0.45 V of voltage.

Automotive Propulsion Simulation Protocol. The protocol's goal is to imitate the functioning of a dynamic vehicle as a representative load for assessing a fuel cell system's power supply capacity. Heavy-duty vehicles, such as buses, employ fuel cells as their power source. The essential factor investigated was the ability to supply hydrogen into the fuel cell as fuel for electrochemical processes within the system at a rate sufficient to meet the need for power. A methodology that typically simulates bus driving behavior is used to compute the electric power requirements. To create the proper test protocol, the bus movement consists of Newton's laws of motion-compliant bus resistance, track curves, gradients, speed restrictions, and modes of operation, and voltage, weight, movement feature, efficiency, auxiliary power, and bus resistance, which are the important parameters of actual vehicle driving, should be concerned.[44] This work addressed dynamic speed cycling and speed constant to design the bus driving simulation protocol and to analyze the functionality of the prototype of the automatic hydrogen flow controller to be able to supply sufficient hydrogen to meet the requirements of the electrochemical reaction. In this research, the driving route in Bangkok during rush hours was selected for measuring the dynamic speed cycling and speed constant. The observed route starts from King Mongkut's University of Technology North Bangkok Station and ends at the Victory Monument Station with a distance of 13.7 km, and this direction includes a total of 39 bus stations and 10 traffic light intersections. The sampling bus was propelled with the highest, average, and lowest speeds of 57.7, 10.8, and 0 km/h, respectively (Figure 13a). In the data collection, selecting a route and time results in data on bus driving behaviors that are constantly changing and at rapid speeds. The data in Figure 13a can be divided into two propulsion modes: speed cycling and speed constant. Figure 13b presents the created protocol for experimental activities.

The designed technique is used to examine the operation of the in-house automatic hydrogen flow controller built into a fuel cell system's power generation capability using a load dynamic test. To fulfill protocol requirements, the hydrogen

https://doi.org/10.1021/acsomega.2c02000
ACS Omega 2022, 7, 38277−38288

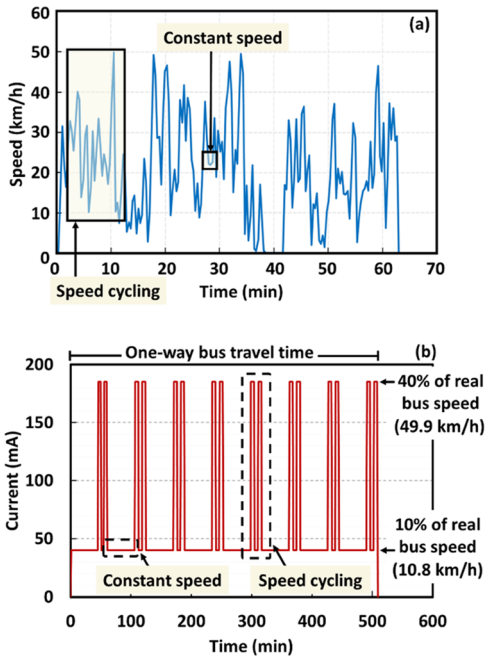

Figure 13. (a) Bus driving behavior model between the KMUTNB Station to the Victory Monument Station and (b) bus driving simulation protocol in central Bangkok.

flow rate can be changed. The primary goal is to investigate the system's gas-feeding capability for electrochemical reactions. The results of polarization curves and Nyquist's curves tested before and after testing fuel cell systems with the aforementioned protocol can be analyzed. The activation loss section of the polarization curve is examined to determine the electron density that can overcome the activation energy values on the anode and cathode sides. The electron density is caused by the oxidation of hydrogen on the anode side catalyst surface. As a result, the amount of hydrogen is an independent variable used in the analysis of this point, as well as the loss due to concentration loss, to determine how quickly the reactants are fed enough to meet the fuel cell's electric power demand. As a result, the data analysis in this section is an examination of the ability to respond to changes in the hydrogen flow rate in a sufficient manner for the electrochemical reactions controlled by the in-house automatic hydrogen flow controller.[21−23] The Nyquist's curve is concerned with the electrochemical reaction characterization of fuel cell systems, which is studied in the midfrequency range to investigate the charge transfer of the reaction corresponding to the extinction part. This is due to the polarization curve's electrochemical reaction, and at low frequencies it represents the diffusion of the reactant into the electrochemical reaction within the system, corresponding to the loss due to the polarization curve's reactant concentration.[24−26] Insights can be obtained from this electrochemical analysis technique for further analysis of the feasibility of implementing the built flow controller.

Design and Installation of the Automatic Hydrogen Flow Controller. The effect of hydrogen fuel content as the main determinant of the electrochemical reaction on the catalyst surface will be investigated using dynamic bus behavior modeling. As a result, the amount of hydrogen needed to complete the electrochemical process changes depending on the vehicle's speed. Furthermore, extra fuel must be used as rarely as possible to attain fuel efficiency. The goal of this experimental activity was to create dynamic performance testing equipment for the fuel cell test station. Figure 14

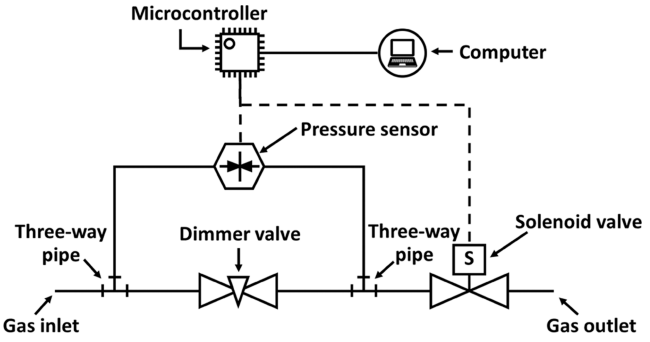

Figure 14. Schematic of the automatic hydrogen flow controller.

depicts the fabricated automatic hydrogen flow controller scheme. The automatic hydrogen flow controller works on the idea that hydrogen flows through the pipe system's hole orifice to create a pressure drop between the pipes across the pressure sensor that is proportionate to the flow rate out of the system. To guarantee that the built-in flow controller is accurate, the resulting flow rate is tested with a commercial flow controller. The voltage is measured by the pressure sensor when hydrogen flows into the system, which converts the analog-to-digital value into the microcontroller while measuring the actual flow rate. The programmable microcontroller provides a calculating function for the user to map the instrument voltage to the measured voltage. The signal must be amplified using an IC instrument amplifier due to the low voltage value. The microcontroller's data is then transferred to the solenoid valve, which opens the hole as programmed.[45] In the event of bus protocols, different energy requirements will be required depending on the dynamics, resulting in varied hydrogen consumption. Furthermore, the solenoid valve's diameter must be increased to allow hydrogen to pass through the operation. As a result of this strategy, the fuel economy will improve.

AUTHOR INFORMATION

Corresponding Author

Rungsima Yeetsorn − *Materials and Production Engineering Program, The Sirindhorn International Thai-German Graduate School of Engineering, King Mongkut's University of Technology North Bangkok, Bangkok 10800, Thailand;* orcid.org/0000-0002-8029-0305; Email: rungsima.y@tggs.kmutnb.ac.th

Authors

Yaowaret Maiket − *Department of Industrial Chemistry, Faculty of Applied Science, King Mongkut's University of Technology North Bangkok, Bangkok 10800, Thailand*

Wattana Kaewmanee − *Thai-French Innovation Institute, King Mongkut's University of Technology North Bangkok, Bangkok 10800, Thailand*

Complete contact information is available at: https://pubs.acs.org/10.1021/acsomega.2c02000

Notes

The authors declare no competing financial interest.

https://doi.org/10.1021/acsomega.2c02000
ACS Omega 2022, 7, 38277−38288

■ ACKNOWLEDGMENTS

The authors would like to express their appreciation for financial support received from King Mongkut's University of Technology North Bangkok, Contract no. KMUTNB-MHESI-64-14.4 and the Thai-French Innovation Institute for the scholarship.

■ REFERENCES

(1) Alvarez-Meaza, I.; Zarrabeitia-Bilbao, E.; Rio-Belver, R. M.; Garechana-Anacabe, G. Fuel-cell electric vehicles: Plotting a scientific and technological knowledge map. *Sustainability* **2020**, *12*, 2334.
(2) Wind, J.Hydrogen-Fueled Road Automobiles—Passenger Cars and Buses. In *Compendium of Hydrogen Energy*, Daimler, A. G., Ed.; Woodhead Publishing: Kirchheim/Teck-Nabern, Germany, 2016; Vol. *4*, pp 3—21.
(3) Thomas, C. E. Fuel cell and battery electric vehicles compared. *Int. J. Hydrogen Energy* **2009**, *34*, 6005—6020.
(4) Ning, F.; He, X.; Shen, Y.; Jin, H.; Li, Q.; Li, D.; Zhou, X.; et al. Flexible and lightweight fuel cell with high specific power density. *ACS Nano* **2017**, *11*, 5982—5991.
(5) Kadyk, T.; Schenkendorf, R.; Hawner, S.; Yildiz, B.; Römer, U. Design of fuel cell systems for aviation: representative mission profiles and sensitivity analyses. *Front. Energy Res.* **2019**, *7*, 35.
(6) Marcinkoski, J.; Vijayagopal, R.; Kast, J.; Duran, A. Driving an industry: medium and heavy duty fuel cell electric truck component sizing. *World Electr. Veh. J.* **2016**, *8*, 78—89.
(7) Sery, J.; Leduc, P. Fuel cell behavior and energy balance on board a Hyundai Nexo. *Int. J. Engine Res.* **2022**, *23*, 709—720.
(8) Yeetsorn, R.; Petrone, R.; Hissel, D.; Harel, F.; Breaz, E.; Gao, F.; Pera, M. C. Influence of cycle repetition on stack voltage degradation during fuel cell stress tests. *Fuel Cells* **2022**, *22*, 85—101.
(9) Mobarra, M.; Rezkallah, M.; Ilinca, A. Variable Speed Diesel Generators: Performance and Characteristic Comparison. *Energies* **2022**, *15*, 592.
(10) Chen, F. Q.; Zhang, M.; Qian, J. Y.; Chen, L. L.; Jin, Z. J. Pressure analysis on two-step high pressure reducing system for hydrogen fuel cell electric vehicle. *Int. J. Hydrogen Energy* **2017**, *42*, 11541—11552.
(11) Alavi, O.; Rajabloo, T.; De Ceuninck, W.; Daenen, M. Non-Isolated DC-DC Converters in Fuel Cell Applications: Thermal Analysis and Reliability Comparison. *Appl. Sci.* **2022**, *12*, 5026.
(12) Ferrara, A.; Jakubek, S.; Hametner, C. Energy management of heavy-duty fuel cell vehicles in real-world driving scenarios: Robust design of strategies to maximize the hydrogen economy and system lifetime. *Energy Convers. Manage.* **2021**, *232*, No. 113795.
(13) Zhang, X. Current status of stationary fuel cells for coal power generation. *Clean Energy* **2018**, *2*, 126—139.
(14) Hwang, J. J.; Hu, J. S.; Lin, C. H. Design of a range extension strategy for power decentralized fuel cell/battery electric vehicles. *Int. J. Hydrogen Energy* **2015**, *40*, 11704—11712.
(15) Janicka, E.; Mielniczek, M.; Gawel, L.; Darowicki, K. Optimization of the Relative Humidity of Reactant Gases in Hydrogen Fuel Cells Using Dynamic Impedance Measurements. *Energies* **2021**, *14*, 3038.
(16) Yeetsorn, R.; Maiket, Y.; Kaewmanee, W. The observation of supercapacitor effects on PEMFC—supercapacitor hybridization performance through voltage degradation and electrochemical processes. *RSC Adv.* **2020**, *10*, 13100—13111.
(17) Yano, M.; Kuroda, E.; Tagami, H.; Kuroda, K.; Watanabe, S. Development of fuel consumption measurement method for fuel cell vehicle-flow method corresponding to pressure pulsation of hydrogen flow. *SAE Trans.* **2007**, *116*, 612—620.
(18) Schober, P.; Vetter, T. R. Two-sample unpaired t tests in medical research. *Anesth. Analg.* **2019**, *129*, 911.
(19) Sheth, S. B.; Sheth, B. R. A variant of the student's t-test for data of varying reliability. *bioRxiv* **2019**, No. 525774.
(20) Limentani, G. B.; Ringo, M. C.; Ye, F.; Bergquist, M. L.; McSorley, E. O. Beyond the t-test: statistical equivalence testing. *Anal. Chem.* **2005**, *77*, 221—226.
(21) Zhang, J.; Hanik, B. W.; Chaney, B. H. Confidence Intervals: Evaluating and Facilitating Their Use in Health Education Research. *Health Educ.* **2008**, *1*, 29—36.
(22) Colin Cameron, A.; Windmeijer, F. A. An R-squared measure of goodness of fit for some common nonlinear regression models. *J. Econom.* **1997**, *77*, 329—342.
(23) Wehkamp, N.; Breitwieser, M.; Büchler, A.; Klingele, M.; Zengerle, R.; Thiele, S. Directly deposited Nafion/TiO 2 composite membranes for high power medium temperature fuel cells. *RSC Adv.* **2016**, *6*, 24261—24266.
(24) Reshetenko, T.; Kulikovsky, A. On the origin of high frequency impedance feature in a PEM fuel cell. *J. Electrochem. Soc.* **2019**, *166*, F1253.
(25) Talj, R.; Azib, T.; Bethoux, O.; Remy, G.; Marchand, C.; Berthelot, E. Parameter analysis of PEM fuel cell hysteresis effects for transient load use. *Eur. Phys. J. Appl. Phys.* **2011**, *54*, No. 23410.
(26) Huang, Y. H.; Hsu, Y. H.; Pan, Y. T. Fabrication of Catalyst Layers with Preferred Mass and Charge Transport Properties through Texture Engineering. *ACS Appl. Energy Mater.* **2022**, *5*, 2890—2897.
(27) Huang, X.; Zhang, Z.; Jiang, J. In *Fuel Cell Technology for Distributed Generation: An Overview*, 2006 IEEE International Symposium on Industrial Electronics; IEEE, 2006; pp 1613—1618.
(28) Cha, H.; Kwon, O.; Kim, J.; Choi, H.; Yoo, H.; Kim, H.; Park, T. Effects of the Anode Diffusion Layer on the Performance of a Nonenzymatic Electrochemical Glucose Fuel Cell with a Proton Exchange Membrane. *ACS Omega* **2021**, *6*, 34752—34762.
(29) Wang, Y.; Wang, L.; Ji, X.; Zhou, Y.; Wu, M. Experimental and Numerical Study of Proton Exchange Membrane Fuel Cells with a Novel Compound Flow Field. *ACS Omega* **2021**, *6*, 21892—21899.
(30) Hoeflinger, J.; Hofmann, P. Air mass flow and pressure optimisation of a PEM fuel cell range extender system. *Int. J. Hydrogen Energy* **2020**, *45*, 29246—29258.
(31) Padha, B.; Verma, S.; Mahajan, P.; Arya, S. Electrochemical Impedance Spectroscopy (EIS) Performance Analysis and Challenges in Fuel Cell Applications. *J. Electrochem. Sci. Technol.* **2022**, *13*, 167—176.
(32) Wang, H.; Yuan, X. Z.; Li, H.*PEM Fuel Cell Diagnostic Tools*; CRC Press: London, 2011; Vol. *2*, pp 1—35.
(33) Sorrentino, A.; Sundmacher, K.; Vidakovic-Koch, T. Polymer electrolyte fuel cell degradation mechanisms and their diagnosis by frequency response analysis methods: a review. *Energies* **2020**, *13*, 5825.
(34) Cruz-Manzo, S.; Rama, P.; Chen, R. The low current electrochemical mechanisms of the fuel cell cathode catalyst layer through an impedance study. *J. Electrochem. Soc.* **2010**, *157*, 400.
(35) Cosse, C.; Schumann, M.; Becker, D.; Schulz, D. Simulation of electric field control effects on the ion transport in proton exchange membranes for application in fuel cells and electrolysers. *Int. J. Hydrogen Energy* **2022**, *47*, 7961—7974.
(36) Kumar, R. R.; Suresh, S.; Suthakar, T.; Singh, V. K. Experimental investigation on PEM fuel cell using serpentine with tapered flow channels. *Int. J. Hydrogen Energy* **2020**, *45*, 15642—15649.
(37) Lobo, R.; Ribeiro, J.; Inok, F. Hydrogen Uptake and Release in Carbon Nanotube Electrocatalysts. *Nanomaterials* **2021**, *11*, 975.
(38) Bénard, P.; Chahine, R. Storage of hydrogen by physisorption on carbon and nanostructured materials. *Scr. Mater.* **2007**, *56*, 803—808.
(39) Miller, J. T.; Meyers, B. L.; Modica, F. S.; Lane, G. S.; Vaarkamp, M.; Koningsberger, D. C. Hydrogen temperature-programmed desorption (H2 TPD) of supported platinum catalysts. *J. Catal.* **1993**, *143*, 395—408.
(40) Li, J.; Hu, Z.; Xu, L.; Ouyang, M.; Fang, C.; Hu, J.; Jiang, H.; et al. Fuel cell system degradation analysis of a Chinese plug-in hybrid fuel cell city bus. *Int. J. Hydrogen Energy* **2016**, *41*, 15295—15310.

https://doi.org/10.1021/acsomega.2c02000
ACS Omega 2022, 7, 38277—38288

(41) Kurtz, J. M.; Sprik, S.; Saur, G.; Onorato, S.*Fuel Cell Electric Vehicle Durability and Fuel Cell Performance (No. NREL/TP-5400-73011)*; National Renewable Energy Lab. (NREL): Golden, CO (United States), 2019.
(42) Miyake, T.; Rolandi, M. Grotthuss mechanisms: from proton transport in proton wires to bioprotonic devices. *J. Phys.: Condens. Matter* **2015**, *2*, No. 023001.
(43) Miyake, T.; Rolandi, M. Grotthuss mechanisms: from proton transport in proton wires to bioprotonic devices. *J. Phys.: Condens. Matter* **2015**, *28*, No. 023001.
(44) Sumpavakup, C.; Kulworawanichpong, T.Multi-Train Movement Simulation Using MATLAB Object-Oriented Programming. In *Applied Mechanics and Materials*; Trans Tech Publications Ltd, 2015; Vol. *763*, pp 153−158.
(45) Zhang, P.*Advanced Industrial Control Technology*, 1st ed.; Andrew, W., Ed.; Elsevier Inc: UK, 2010; pp 1−841.

https://doi.org/10.1021/acsomega.2c02000
ACS Omega 2022, 7, 38277−38288